

Analysis of $\text{Li}^6(\text{Li}^6, \alpha)\text{Be}^8$ at 3.4 MeV*

J. HOWARD SHAFER†

Reed College, Portland, Oregon

Angular distributions for alpha particles from $\text{Li}^6(\text{Li}^6, \alpha)\text{Be}^8$ have been obtained from five distinct alpha-particle peaks. However, only one peak, that corresponding to the 2.90-MeV state of Be^8 , has been positively identified. An analysis of the Li^6+Li^6 gamma-ray spectrum with 100 times more counts than previous data indicate that no gamma ray from Be^8 exists with an intensity greater than $2 \times 10^{-6}\%$ that of the 6.90-MeV peak from C^{11} and B^{11} . This indicates an $\alpha+d$ configuration for Li^6 . The experiment has been performed with a Van de Graaff accelerator.

I. INTRODUCTION

THE large number of nucleons in lithium relative to the height of the Coulomb barrier and the high mass excess make lithium a very useful projectile for nuclear spectroscopic studies. In recent years, much research has been done on reactions involving light nuclei, using such accelerated lithium-ion beams.¹⁻⁸ Several experiments have dealt with the reaction $\text{Li}^6(\text{Li}^6, \alpha)\text{Be}^8$. Because no gamma rays from this reaction have been observed, particle-detection methods were necessary. Accelerator energies up to 5 MeV have been used.^{6,9-11}

In the present experiment, the angular distributions of alpha particles from Li^6+Li^6 have been measured for all alpha particles over 5.6 MeV, using an accelerator energy of 3.4 MeV. Gamma rays over 8 MeV have also been studied to determine the yield from odd J ($T=1$) energy levels of Be^{8*} .

II. EXPERIMENTAL METHOD

A thin Li^6F target on a 3.1-mg/cm² Al backing and a 3.4-MeV Li^{6+} ion beam from the State University of Iowa Van de Graaff accelerator were used throughout the experiment. A solid-state particle detector, used with standard electronics, measured particle spectra between $2\frac{1}{2}^\circ$ and $142\frac{1}{2}^\circ$ in the laboratory system. The detector

was mounted 2.54 cm from the target and was 5° wide with respect to the scattered particles.

Aluminum foils of several thicknesses were set in front of the particle detector, and the tables by Whaling¹² were used to determine energy losses through the foils. The original purpose of this was to facilitate the measurement of very low-energy alpha particles by measuring the energy losses of the particles due to the foils. However, it was quickly discovered that these low-energy alpha particles could not be seen at all. Nevertheless, it is thought that errors in the estimates of foil thicknesses are random, and that these errors were probably minimized through the comparison of results

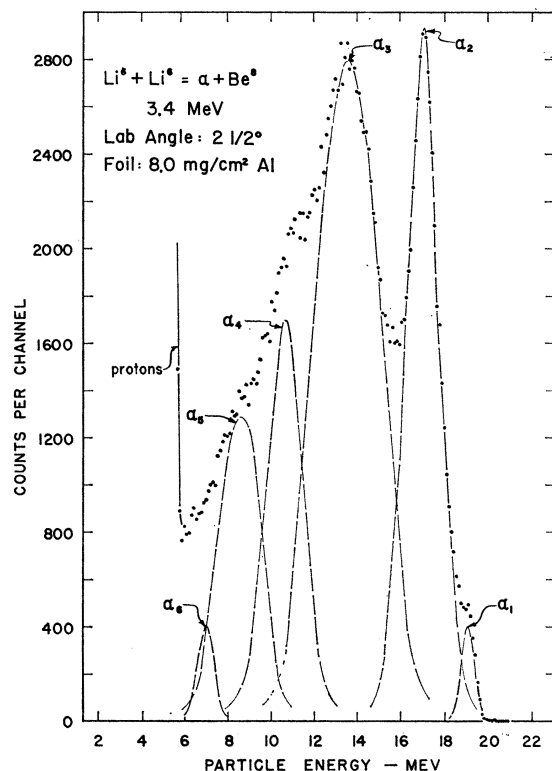


FIG. 1. Li^6+Li^6 particle spectrum at $2\frac{1}{2}^\circ$ in the lab system. Only alpha particles appear above 5.6 MeV. Alpha peaks 4 and 5 are indicated by abrupt changes in the slope of the low-energy edge of peak 3. Alpha peak 6 is not considered real.

* Work supported by the Hill Foundation and the State University of Iowa.

† Present address: University of Colorado, Boulder, Colorado.

¹ E. H. Berkowitz, Phys. Rev. **126**, 2168 (1962).

² E. Norbeck, Jr., and C. S. Littlejohn, Phys. Rev. **108**, 754 (1957).

³ R. L. McGrath, Phys. Rev. **127**, 2138 (1962).

⁴ J. M. Blair, *Reactions between Complex Nuclei*, edited by A. Zucker, F. T. Howard, and E. R. Halbert (John Wiley & Sons, Inc., New York, 1960), p. 138.

⁵ G. C. Morrison and M. N. Huberman, *Reactions between Complex Nuclei*, edited by A. Zucker, F. T. Howard, and E. C. Halbert (John Wiley & Sons, Inc., New York, 1960), p. 246.

⁶ G. C. Morrison, in *Direct Interactions and Nuclear Reaction Mechanisms*, edited by E. Clementel and C. Villi (Gordon and Breach, Science Publishers, New York, 1963), p. 878.

⁷ M. N. Huberman, M. Kamegai, and G. C. Morrison, Phys. Rev. **129**, 791 (1963).

⁸ R. R. Carlson and E. Norbeck, Jr., Phys. Rev. **131**, 1204 (1963).

⁹ M. Coste and L. Marquez, Compt. Rend. **254**, 1768 (1962).

¹⁰ M. Coste and F. Perrin, Compt. Rend. **255**, 2138 (1963).

¹¹ C. Lemeille, D. Manesse, L. Marquez, N. Saunier, and J. L. Quebert, Colloque de Physique Nucléaire, Orsay, France, 1963 (unpublished).

¹² W. Whaling, in *Handbuch der Physik*, edited by S. Flügge (Springer-Verlag, Berlin, 1952), Vol. 34, pp. 193-217.

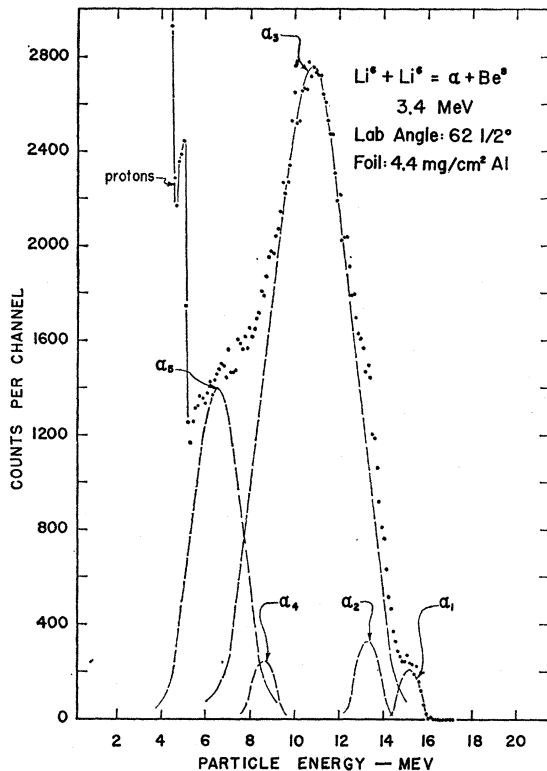


FIG. 2. Li^6+Li^6 particle spectrum at $62\frac{1}{2}^\circ$ in the lab system. Alpha peaks 2 and 4 have been found by comparing the shapes of alpha peaks 3 and 5 with those from closely adjacent angles.

obtained with several foils. This is important because the target backing could not be removed and most measurements had to be corrected for it.

A 3-in.-diam NaI(Tl) crystal set at 135° with respect to the incident Li^{6+} beam monitored gamma rays for the normalization of particle data. However, a larger, 12.5-cm-diam by 15.0-cm-long NaI(Tl) crystal set at 90° to the incident beam measured the gamma-ray spectrum analyzed in the experiment. This second crystal was set about 5.1 cm from the target. The 1.6-mm-thick brass target-chamber wall and the 0.75-mm-thick aluminum can containing the crystal were the only obstructions between the target and the NaI(Tl) detector.

The large crystal and the semiconductor particle detector were each used with separate 256-channel pulse-height analyzers.

Because the Q value for $\text{Li}^6(\text{Li}^6, \alpha)\text{Be}^8$ (20.784 MeV) is almost twice as high as the next Q value (12.209 MeV for $\text{Li}^6(\text{Li}^6, p)\text{B}^{11}$), special techniques were not necessary to identify alpha particles above 12 MeV. By lowering the particle-detector bias voltage sufficiently, protons were prevented from dissipating more than 5.6 MeV in the detector. Thus, all alpha particles above this energy could be easily identified.

Figures 1-3 show typical particle spectra. To analyze these spectra, it was assumed that the alpha-particle

peaks were symmetric with respect to their high- and low-energy edges. The low-energy edge of the most energetic peak was matched with its visible high-energy edge, and the resulting distribution was then subtracted from the spectrum to reveal the high-energy side of the next peak. As a certain amount of guess work is always involved in such a method, the lower-energy peaks contain much more error than those of higher energy. The fluctuation in peak width, which can be noted in the figures, is most probably due to this subtraction process, although it does not always appear completely random. This is especially true of alpha peak No. 3. This peak width has a maximum at about 30° and minima at about 0° and 120° in the lab system. The individual peaks are indicated by dashed lines in Figs. 1-3.

III. EXPERIMENTAL RESULTS

Figure 4 shows the alpha-particle peak energy as a function of laboratory angle. Points from six alpha-particle distributions are included. The solid lines on the graph are calculated from the kinematics for alpha particles resulting from Be^8 being formed in the ground state, the 2.90-MeV state and the 11.4-MeV state. The break in the experimental curves between 80° and 90° has not been explained, but the excellent fit of the second

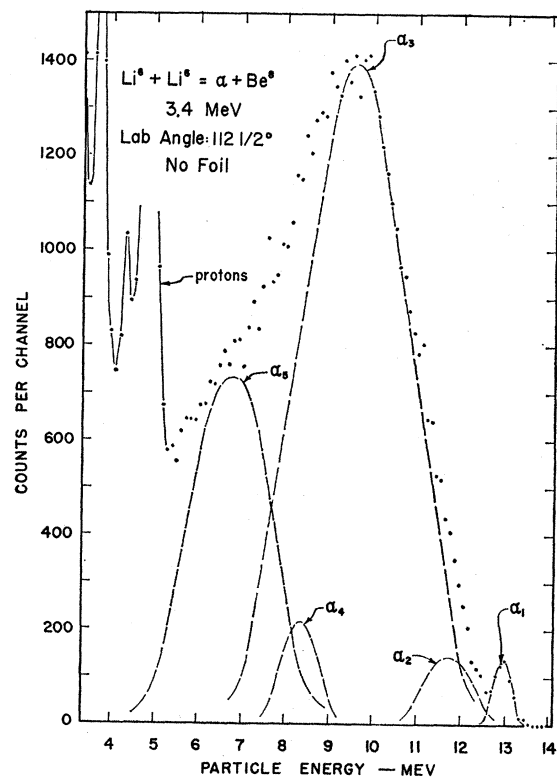


FIG. 3. Li^6+Li^6 particle spectrum at $112\frac{1}{2}^\circ$ in the lab system. Note that the scales are not the same as in Figs. 1 and 2. Alpha peaks 2 and 4 have been found by comparing the shapes of alpha peaks 3 and 5 with those from closely adjacent angles.

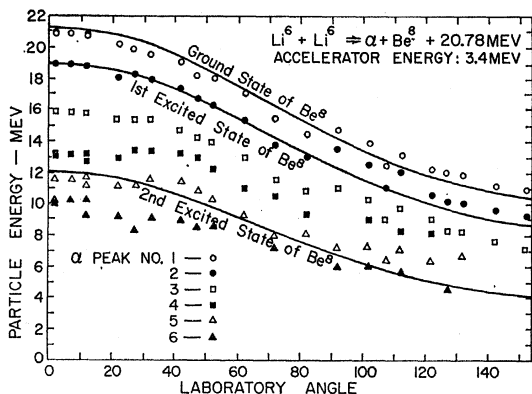


FIG. 4. Alpha-particle energies in the lab system. Several of the peaks do not fit the latest energy-level diagrams of Be⁸. The break in the curves at 90° has not been explained. This figure is explained more completely in the text.

alpha-particle distribution (alpha peak No. 2) indicates the validity of these curves for angles less than 90°. Moreover, the curves have the correct kinematic shape at all angles.

Figures 5-10 show the experimental angular distributions of the relative intensities of these distributions in the center-of-mass system. Because target and bombarding particles are identical, they should be symmetrical about 90°, and in order to exhibit deviations

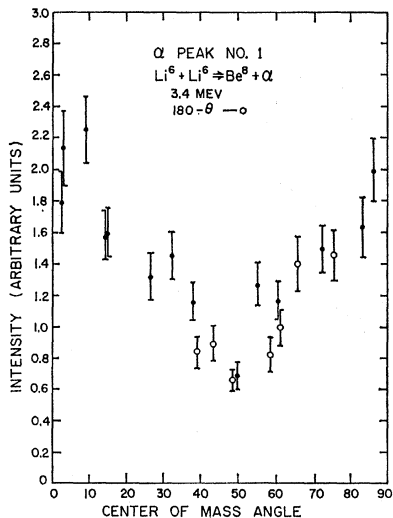


FIG. 5. The angular distribution of alpha particles from alpha peak 1. This appears to have symmetry about 90° and also about 45°.

from this symmetry most advantageously, intensities at angles θ greater than 90° have been graphed as $180^\circ - \theta$.

A summary of the results follows.

A. Alpha Peak No. 1

This peak is most probably due to the ground state of Be⁸. In fact, Coste and Perrin¹⁰ have identified a very similar peak with the ground state. However, according to Fig. 4, it is about 0.4 MeV above ground. Its meas-

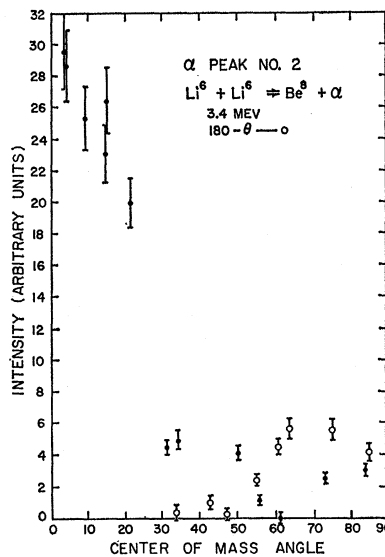


FIG. 6. The angular distribution of alpha particles from alpha peak 2. The forward peaking indicates a stripping reaction. An asymmetry about 90° is apparent.

ured, uncorrected width of 0.7 ± 0.2 MeV is much in excess of the 2.5-eV ground-state width listed by Ajzenberg-Selove and Lauritsen.¹³ The angular distribution (Fig. 5) is similar to that found by Coste and Perrin at a lower energy.

B. Alpha Peak No. 2

According to Fig. 4, this peak corresponds to the 2.90-MeV level of Be⁸. Its measured, uncorrected width of 1.4 ± 0.3 MeV compares favorably with 1.46 ± 0.05 MeV which is listed by Ajzenberg-Selove and Lauritsen.¹⁴ It has been noted that this was not at all the case

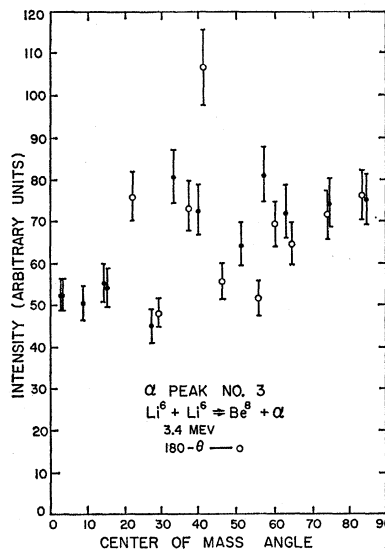


FIG. 7. The angular distribution of alpha particles from alpha peak 3. The distribution is vaguely isotropic. The wide scattering of points does not seem compatible with the prominence of this peak, but it is most likely due to the uncertainty in subtractions on its low-energy side.

¹³ F. Ajzenberg-Selove and T. Lauritsen, Nucl. Phys. **11**, 44 (1959).

¹⁴ F. Ajzenberg-Selove and T. Lauritsen, Nucl. Phys. **11**, 44 (1959).

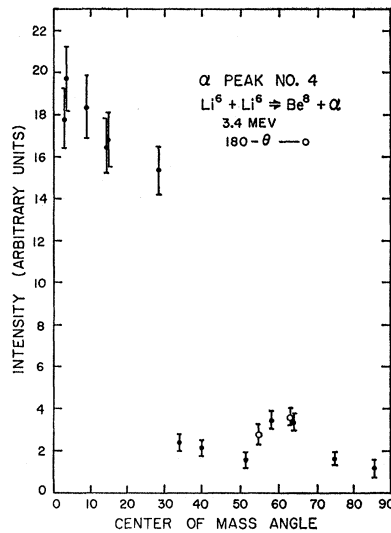


FIG. 8. The angular distribution of alpha particles from alpha peak 4. A stripping reaction is indicated.

with alpha peak No. 1. No attempt was made to determine the magnitude of instrumental peak width, but the very close agreement of both the energy and the width of alpha peak No. 2 with other experiments poses a question about the general lack of agreement of these measurements on alpha peak No. 1. The angular distribution (Fig. 6) would seem to indicate some kind of double-stripping mechanism, although the energy is low for such a reaction. An asymmetry about 90° is also apparent. Although it may be real, it is most probably the result of the method of data reduction.

C. Alpha Peak No. 3

This peak has been attributed to the disintegration $\text{Be}^{8*} = 2\alpha$, where Be^{8*} is in a 20.4-MeV state.⁹ According to Fig. 4, it might be due to a 6.5 ± 0.2 -MeV level in Be^8

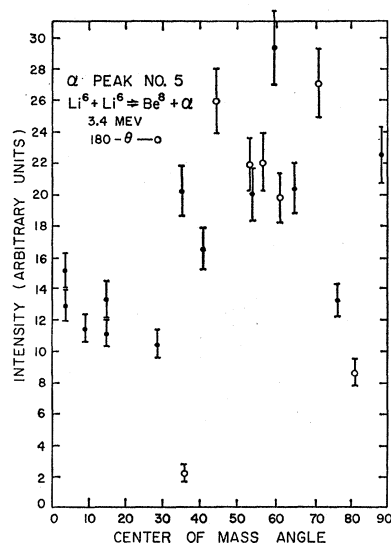


FIG. 9. The angular distribution of alpha particle from alpha peak 5. The wide scattering of data is a result of uncertainties in the subtraction process used to obtain the peak.

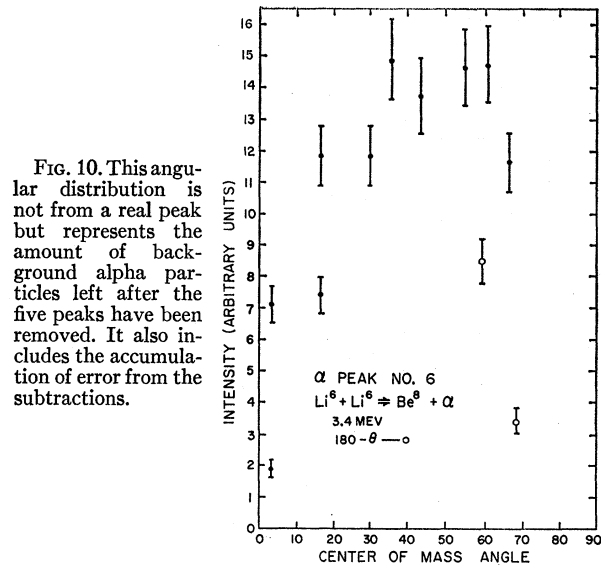


FIG. 10. This angular distribution is not from a real peak but represents the amount of background alpha particles left after the five peaks have been removed. It also includes the accumulation of error from the subtractions.

with a width of 3.4 ± 0.3 MeV. It is also possible that the peak is not symmetric at all, and that it is actually due to a more complex form of reaction such as $\text{Li}^6 + \text{Li}^6 = 3\alpha$. In this case, parts of the lower energy peaks also belong to it, making the analysis very difficult unless it can first be separated from the other alpha-particle peaks.

D. Alpha Peak No. 4

Figure 4 indicates that this peak could be from a 9.5 ± 0.3 -MeV level in Be^8 with a width of 1.5 ± 0.3 MeV. A poorly resolved 10-MeV level with a width of about 1.7 MeV was reported in 1941,¹⁵ but it has not been included in the latest energy-level diagrams of Be^8 .¹² The angular distribution (Fig. 8) indicates a stripping reaction even though the method of subtraction used to obtain this peak would tend to introduce quite large errors.

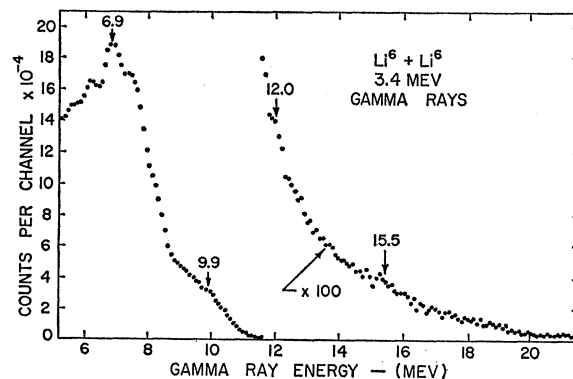


FIG. 11. High-energy gamma rays from $\text{Li}^6 + \text{Li}^6$. No Be^8 gamma ray with more than $2 \times 10^{-5}\%$ of the 6.90-MeV gamma-ray peak intensity is seen.

¹⁵ H. T. Richards, Phys. Rev. 59, 796 (1941).

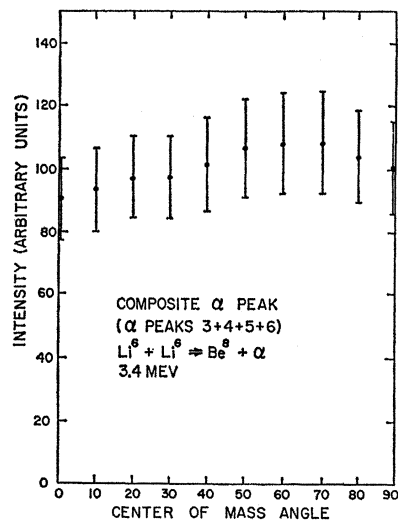


FIG. 12. This alpha-particle angular distribution is a summation of the last 4 alpha-particle peaks. The distribution is almost isotropic.

E. Alpha Peak No. 5

This peak, according to Fig. 4, most likely corresponds to the 11.4-MeV state of Be^8 , but its measured width is only 2.1 ± 0.4 MeV which is much less than the 6-MeV width reported elsewhere.¹³ The true width, as well as the actual size, may be obscured by a large alpha-particle background. The angular distribution (Fig. 9) is rather vague.

F. Alpha Peak No. 6

This is probably due to the alpha-particle background from $\text{Be}^{8*} = 2\alpha$ or from the tail of alpha peak No. 3. The angular distribution (Fig. 10) has been included to give an indication of the magnitude of the background and because it was used in estimating the total yield of Be^8 from the reaction.

G. Gamma-Ray Spectrum

Figure 11 shows the gamma-ray spectrum from $\text{Li}^6 + \text{Li}^6$ above 6 MeV. The 6.90-MeV peak due to C^{11} and B^{11} is 190 000 counts high as compared with 1800 counts for the analysis done by Berkowitz.¹ Although escape peaks, etc., have obscured detail, the following is observed above 9 MeV.

A bulge at about 9.9 MeV probably contains at least one peak, but its identification is uncertain. B^{11} , C^{11} , and C^{12} all have energy levels in this region. The clearest peak is at about 12 MeV and apparently corresponds to the 12.3-MeV level of C^{11} . A slight bump at about 15.5 MeV, which is probably above background, might correspond to levels of C^{12} , B^{11} , C^{11} , or Be^8 , but the best fits are C^{12} (15.62 MeV), B^{11} (15.76 MeV), and C^{11} (15.7 MeV). It is not known if any of these levels actually decay through gamma-ray channels.

According to these data, it appears unlikely that any gamma-ray exit channel from Be^8 exists more intense

than $2 \times 10^{-5}\%$ of the 6.90-MeV peak intensity. Therefore, Be^8 seems to decay only through particle emission in this reaction. Because the odd- ($T=1$) spin states of Be^8 can decay only via gamma-ray channels, these states appear not to be populated. Odd-spin states would be formed through the transfer of uncoupled neutron-proton pairs, leading to the conclusion that only neutron-proton pairs coupled in a deuteron configuration are transferred; i.e., Li^6 behaves here as if it were $\alpha + d$.

H. Total Be^8 Yield from $\text{Li}^6 + \text{Li}^6$

A particle spectrum from $12\frac{1}{2}^\circ$ in the lab system has been analyzed to estimate the percentage yield of Be^8 compared to the other reaction products. If most of the alpha particles from the reaction are present in the six measured distributions, and if each alpha particle represents one Be^8 nucleus, then the Be^8 yield for this particular run is $(22 \pm 6)\%$. Figure 12, which is the angular distribution of a composite of practically all of the alpha particles measured, indicates that the total yield is almost isotropic. Therefore, if the yields from the other exit channels are also fairly isotropic, the Be^8 yield for the reaction is $(22 \pm 6)\%$ of the total yield. However, if alpha peak No. 3 has been incorrectly analyzed, it is possible that a great part of the reaction proceeds: $\text{Li}^6 + \text{Li}^6 = 3\alpha$. In this case, there are three alpha particles for each reaction so that the yield is only about one-third as great. This is about $(7 \pm 2)\%$.

Figure 13, which has been obtained from Berkowitz,¹⁶ shows the relative yields that he has obtained for $\text{Li}^6 + \text{Li}^6$ using gamma-ray techniques. The two possible yields from the present experiment have been added. Because it seems most likely that the alpha-particle exit channel is the result of the exchange of a deuteron between the two incident nuclei, and because the results of the gamma-ray measurements indicate that the removal of a deuteron from one of the nuclei is a very likely mechanism, the yield for $\text{Li}^6 + \text{Li}^6 = 3\alpha$ appears too low to be likely. On the other hand, if it is noted that Be^8 has only even parity states at the energies involved, so that it cannot be created from $\text{Li}^6 + \text{Li}^6$

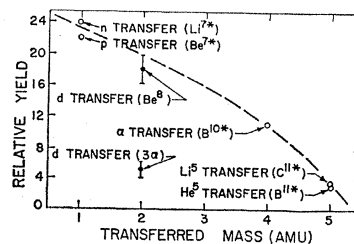


FIG. 13. Reaction product yields from $\text{Li}^6 + \text{Li}^6$ taken from gamma-ray data versus mass transferred per reaction. If Be^8 is always formed in a deuteron transfer, the Be^8 yield falls almost on a smooth curve with the other reaction products. The $\alpha + d$ configuration of Li^6 indicates the Be^8 yield should be large.

¹⁶ E. H. Berkowitz (private communication).

where odd relative angular momenta are involved, then the yield indicated in Fig. 13 for the reaction producing Be^8 is about where it might be expected on a qualitative basis.

IV. CONCLUSION

The alpha-particle spectra from Li^6+Li^6 contain irregularities which are not yet fully explained. Of special interest is the mechanism involved in the production of alpha peak No. 3. The gamma-ray spectrum

indicates a singular lack of the ($T=1$) states of Be^8 which can be explained by assuming that Li^6 is in the form $\alpha+d$.

ACKNOWLEDGMENTS

A great deal of thanks is extended to Dr. K. E. Davis for the help that he has given in the preparation of this material. Also, Dr. E. Norbeck, Jr., and E. Berkowitz are to be acknowledged for their help and suggestions which made this work possible.

Slow Neutron Cross Sections for He^3 , B, and Au

J. ALS-NIELSEN AND O. DIETRICH

The Danish Atomic Energy Commission, Research Establishment Risø, Roskilde, Denmark

(Received 20 September 1963)

The He^3 neutron cross section was measured for neutron energies from 0.0003 to 11 eV. In this energy region no deviation from the $1/v$ law can be found from the data. The cross section at 2200 m/sec was found to be $\sigma(\text{He}^3) = 5327_{-9}^{+10}$ b. As an instrumental check the cross sections of natural boron and of gold were also measured and the results agree with the most accurate existing data. The absorption cross sections at 2200 m/sec were found to be $\sigma_a(\text{B}) = 759.1 \pm 2.0$ b and $\sigma_a(\text{Au}) = 98.6 \pm 0.2$ b.

1. INTRODUCTION

THE total neutron cross section of He^3 was measured for neutron energies from 0.0003–11 eV to obtain more accurate data than available until now.¹

As an instrumental check the total cross sections of Au and B were also measured and compared with values obtained in other laboratories.^{2–4} There were two purposes for the measurement of the He^3 cross section: To show that He^3 might be the best primary standard material for neutron standardization, and for use in determination of the absolute efficiency of a He^3 counter.

The most important property of a standard material is that it possesses an accurately measurable $1/v$ absorption cross section (no resonances). This can generally be deduced from the total cross section by subtraction of the scattering cross sections.

Gold and boron have mainly been used as primary standards, but these both entail some disadvantages.

The major disadvantage of gold is a strong resonance at 4.9 eV; and furthermore the correction for the scattering cross sections (especially the incoherent part) is not too accurate.²

The chemical properties of boron imply that the sample must generally be a compound, of which the scattering cross section is rather inaccurately determined for thermal neutron energies on account of the chemical binding.⁵ The determination of the B^{10} density is quite complicated and requires an accurate measurement of the isotopic and chemical compositions in the sample.

He^3 is in practice not seriously contaminated by He^4 , the cross section of which is also very small. Being a monoatomic gas, no coherence effects from chemical bindings or from lattice configuration can take place. Up to at least 10 eV no trace of resonances has been observed. The cross section is of such a size that a sample length of roughly 10 cm, at a pressure of 1 atm, gives suitable transmission for thermal neutrons, and therefore the determination of the He^3 density consists of a straightforward pressure and temperature measurement and a sample length measurement. All these properties qualify He^3 as an excellent material for neutron cross section standardization.

In a He^3 proportional counter of proper geometry, the absolute efficiency in a neutron beam can be determined very accurately. The detection efficiency, i.e., the ratio between the number of (n, p) processes and the number of counts, can be determined with an accuracy of better than 0.3%,⁶ and, by measuring the He^3 pressure carefully and knowing the (n, p) cross section, the absolute

¹ L. D. P. King and L. Goldstein, *Phys. Rev.* **75**, 1366 (1949).

² F. T. Gould, T. I. Taylor, W. W. Havens, Jr., B. M. Rustad, and E. Melkonian, *Nucl. Sci. Eng.* **8**, 453 (1960).

³ A. Deruytter, G. Debus, K. Lauer, H. Moret, and A. Prodocimi, *EUR. J.* **12**, e, 1962 (unpublished).

⁴ G. J. Safford, T. I. Taylor, B. M. Rustad, and W. W. Havens, Jr., *Phys. Rev.* **119**, 1291 (1960); *Nucl. Sci. Eng.* **9**, 99 (1961).

⁵ P. A. Egelstaff, *J. Nucl. Energy* **5**, 41 (1957).